WILEY

Tracking the cargo of extracellular symbionts into host tissues with correlated electron microscopy and nanoscale secondary ion mass spectrometry imaging

Stephanie K. Cohen[1] | Marie-Stéphanie Aschtgen[2] | Jonathan B. Lynch[3] | Sabrina Koehler[3] | Fangmin Chen[3] | Stéphane Escrig[1] | Jean Daraspe[4] | Edward G. Ruby[3] | Anders Meibom[1,5] | Margaret McFall-Ngai[3] [iD]

[1]Laboratory of Biological Geochemistry, École Polytechnique Fédérale de Lausanne (EPFL), Lausanne, Switzerland

[2]Department of Medical Microbiology and Immunology, University of Wisconsin—Madison, Madison, Wisconsin

[3]Kewalo Marine Laboratory, University of Hawaiʻi at Mānoa, Honolulu, Hawaiʻi

[4]Electron Microscopy Facility, University of Lausanne, Lausanne, Switzerland

[5]Center for Advanced Surface Analysis, Institute of Earth Sciences, University of Lausanne, Lausanne, Switzerland

Correspondence
Margaret McFall-Ngai, Kewalo Marine Laboratory, University of Hawaiʻi at Mānoa, 41 Ahui Street, Honolulu, HI 96813.
Tel: (808) 956 8838;
Fax: (808) 956 4768.
Email: mcfallng@hawaii.edu

Anders Meibom, Laboratory of Biological Geochemistry, École Polytechnique Fédérale de Lausanne, EPFL ENAC IIE LGB Station 2, Lausanne CH-1015, Switzerland.
Tel: +41 21 693 80 15.
Email: anders.meibom@epfl.ch

Present address
Stephanie K. Cohen, MyBiotics Pharma Ltd., Plaut Menahem 10, Rehovot 7670609, Israel

Marie-Stéphanie Aschtgen, Department of Microbiology, Tumor and Cell Biology, Karolinska Institutet, Stockholm 171 76, Sweden

Jonathan B. Lynch, Department of Integrative Biology and Physiology, University of California, Los Angeles, Los Angeles, CA

Sabrina Koehler, Kiel Evolution Center, Kiel University, Am Botanischen Garten 1-9, Kiel 24118, Germany

Fangmin Chen, Liaoning Key Lab of Urban Integrated Pest Management and Ecological Security, Shenyang University, Shenyang, Liaoning 110044, China

Abstract

Extracellular bacterial symbionts communicate biochemically with their hosts to establish niches that foster the partnership. Using quantitative ion microprobe isotopic imaging (nanoscale secondary ion mass spectrometry [NanoSIMS]), we surveyed localization of ^{15}N-labelled molecules produced by the bacterium *Vibrio fischeri* within the cells of the symbiotic organ of its host, the Hawaiian bobtail squid, and compared that with either labelled non-specific species or amino acids. In all cases, two areas of the organ's epithelia were significantly more ^{15}N enriched: (a) surface ciliated cells, where environmental symbionts are recruited, and (b) the organ's crypts, where the symbiont population resides in the host. Label enrichment in all cases was strongest inside host cell nuclei, preferentially in the euchromatin regions and the nucleoli. This permissiveness demonstrated that uptake of biomolecules is a general mechanism of the epithelia, but the specific responses to *V. fischeri* cells recruited to the organ's surface are due to some property exclusive to this species. Similarly, in the organ's deeper crypts, the host responds to common bacterial products that only the specific symbiont can present in that location. The application of NanoSIMS allows the discovery of such distinct modes of downstream signalling dependent on location within the host and provides a unique opportunity to study the microbiogeographical patterns of symbiotic dialogue.

KEYWORDS

^{15}N-labeled bacteria, host–microbe communication, squid–vibrio

1 | INTRODUCTION

In 2000, Pascale Cossart, with coauthors Patrice Boquet, Staffan Normark, and Rino Rappuoli, published the book *Cellular Microbiology* (Cossart, 2000). The premise of this timely masterwork was that interactions of bacteria with eukaryotic cells provide a window into the basic mechanisms underlying cell biology. Then, in 2018, in response to the new discoveries enabled by technological advances in nucleic acid sequencing and genetic manipulation, Cossart contributed *The New Microbiology: From Microbiomes to CRISPR* (Cossart, 2018). Implicit in both of these benchmark contributions is the recognition that eukaryotic cells have over evolutionary time always interacted with an astounding diversity of Bacteria and Archaea, and such relationships have shaped all aspects of biology, from the molecular to the ecological. Relevant here is that, within this backdrop of billions of years of microbe–microbe communication, animals radiated over the last ~14% of the biosphere's history, with all 37 recognised animal body plans diverging in the microbe-rich oceans (McFall-Ngai et al., 2013). Despite this circumstance, it has only been recently that animal biologists, who have focused historically almost exclusively on abiotic forces (e.g., temperature, salinity, and oxygen concentration), have recognised that microbes are more than potential pathogens or a food source; rather, they are critical elements of nested communication systems that have been key drivers of animal form and function. This contribution, using nanoscale secondary ion mass spectrometry (NanoSIMS) technology to trace symbiont-derived biomolecules within host cells, explores aspects of communication between the Gram-negative luminous bacterium *Vibrio (Aliivibrio) fischeri* and its host animal, the Hawaiian bobtail squid, *Euprymna scolopes*.

Similar to many microbial partners, such as those in humans, the symbiont *V. fischeri* is (a) horizontally transmitted, that is, acquired by the host from the environment anew each generation (Bright & Bulgheresi, 2010), and (b) resides persistently in extracellular populations in circumscribed microbiogeographical host locations (Donaldson, Lee, & Mazmanian, 2016; Sycuro, Ruby, & McFall-Ngai, 2006). The squid–vibrio symbiotic organ (also referred to as the light organ) association allows for detailed analyses of mechanisms by which specific tissues create niches to promote establishment and persistence of symbiosis, notably the spatio-temporal relationships of the colonisation process (Figure 1; for review, see McFall-Ngai, 2014a; McFall-Ngai, 2014b). During establishment of this symbiosis, a complex series of events takes place over a few hours and across a symbiont migration pathway of ~150 μm with six biochemically and physically distinct regions.

During embryogenesis, the host animal develops a nascent symbiotic organ (Figure 1a) poised to engage symbiont cells, which occur at about ~10^3 cells ml^{-1} of seawater, within minutes after the host hatches from the egg (Montgomery & McFall-Ngai, 1993). The juvenile organ has elaborate ciliated epithelial fields on its lateral faces that interact directly with the seawater environment to recruit *V. fischeri* from the bacterioplankton (Figure 1b; Nawroth et al., 2017). Shortly after hatching, the superficial epithelium sheds mucus in a non-specific response to environmental peptidoglycan (Nyholm, Deplancke, Gaskins, Apicella, & McFall-Ngai, 2002). Some Gram-negative bacteria, particularly the Vibrionaceae, will attach to the cilia and form aggregates of cells on the organ surface (Koehler et al., 2018), but eventually, the symbiont shows competitive dominance. In studies with *V. fischeri* strain ES114, small aggregates of ~5 symbiont cells attach to the host ciliated surface and signal their presence across the ~10,000 cells of the host organ (Altura et al., 2013; Kremer et al., 2013). This signalling changes host gene expression, altering the biochemistry of the host organ's mucociliary environment to favour *V. fischeri* and establishing a chitobiose gradient that attracts *V. fischeri* cells into the organ. Important for the work presented here are the findings that, with *V. fischeri* absent: (a) although the host is interacting with ~10^6 per ml non-specific environmental bacteria, no change in host gene expression is induced (Kremer et al., 2013), and (b) no non-specific bacterial cells migrate into the organ (Nyholm & McFall-Ngai, 2004). Thus, evolutionary selection on host–symbiont communication has resulted in highly refined mechanisms of recognition and specificity that ensure fidelity of the relationship across generations.

During the embryonic period, the host also develops the migration pathway (Figure 1b; Montgomery & McFall-Ngai, 1993). After aggregating on the surface, *V. fischeri* cells enter three pores on either side of the light organ. Each pore leads to an independent crypt where the symbionts will reside. To reach the crypts, the symbiont cells migrate into a pore and through a ciliated duct and antechamber, which are separated from a crypt by a narrow bottleneck (Sycuro et al., 2006). Regardless of the aggregation size and how many *V. fischeri* cells migrate into host the ducts and antechambers, on average, only a single *V. fischeri* cell successfully grows out to populate each of the six crypts (Figure 1c; Bongrand & Ruby, 2018; Wollenberg & Ruby, 2009). Within the crypts, the symbiont cells interface with a microvillous epithelium. In addition, they are restricted to the crypt spaces except with the venting of ~90% of the population each day at dawn (Graf & Ruby, 1998), when symbionts expelled from the crypts pass back through the migration pathway to enter into the bacterioplankton.

Upon colonisation, symbionts induce developmental changes in the animal from the crypt spaces (for review, see McFall-Ngai, 2014b; Moriano-Gutierrez et al., 2019). Each region along the light-organ migratory pathway has its own biomechanical and biochemical signature, which changes upon symbiont of the crypts. Most dramatic is the symbiosis-induced loss of the light-organ superficial ciliated fields that potentiate initial. At ~12 hr following first association with *V. fischeri*, derivatives of symbiont lipopolysaccharide and peptidoglycan induce an irreversible signal of widespread haemocyte (blood cell) trafficking and cell death of the ciliated epithelia that results in their complete loss
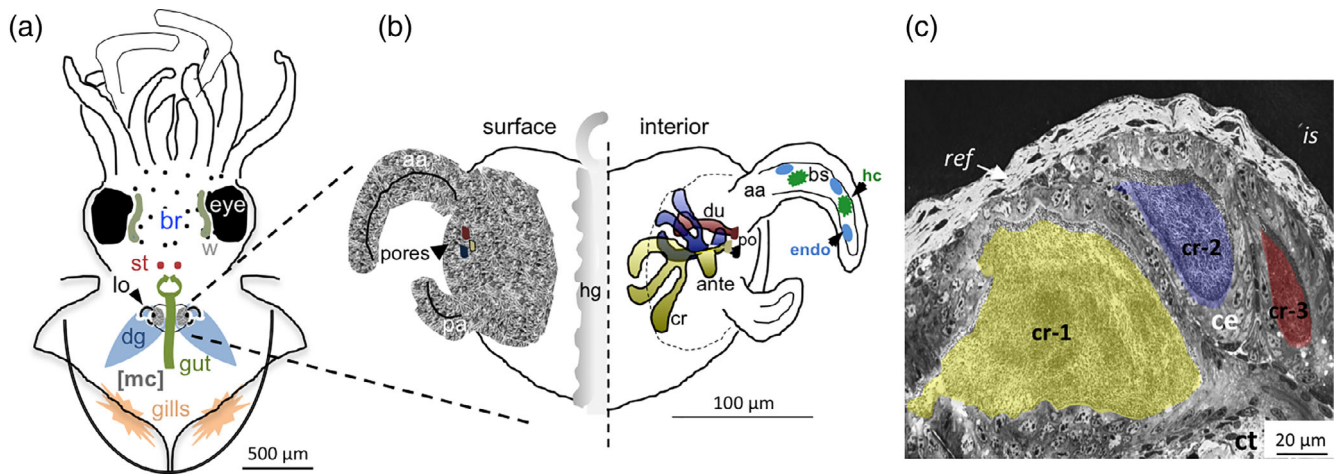
FIGURE 1 Relevant morphology, anatomy, and ultrastructure of the host, *Euprymna scolopes*. (a) A diagram of a ventral dissection revealing the mantle cavity with relevant tissues and organs that were examined in this study. br, brain; dg, digestive gland; lo, light organ; mc, mantle cavity; st, statolith; w, white body. (b) A diagram of the bilateral light organ. Relevant surface features (left half) include the juvenile-specific ciliated epithelium with two appendages, anterior (aa) and posterior (pa), and the field of cilia surrounding three pores. Relevant interior features include the three independent regions of symbiont migration and residence. ante, antechamber diverticulum; bs, blood sinus; cr, crypt; du, duct; endo, endothelial cells lining the blood sinus; hc, haemocytes; po, pores. (c) A transmission electron microscopy with symbiont-containing crypt region of the light organ, false coloured to correspond to coloured regions in (b). cr-1–3, crypts 1–3; ce, crypt epithelium; ct, connective tissue; *is*, ink sac; *ref*, reflector

over 4–5 days. These microbe-associated molecular patterns (MAMPs) are presented to the host crypt epithelia as either freely exported molecules (Koropatnick et al., 2004) or molecules delivered in outer membrane vesicles (OMVs; Aschtgen et al., 2016; Aschtgen, Wetzel, Goldman, McFall-Ngai, & Ruby, 2016). Further, from the crypt spaces, the symbionts induce transcriptomic changes in remote tissues, such as the eyes and gills (Moriano-Gutierrez et al., 2019).

Whereas host receptor/symbiont ligand interactions (e.g., MAMPs and pattern recognition receptors) driving these specific developmental events have been extensively studied (for reviews, see McFall-Ngai, Heath-Heckman, Gillette, Peyer, & Harvie, 2012; Nyholm & Graf, 2012), many other communication networks have been suggested by "-omics" studies (Chun et al., 2008; Kremer et al., 2013; Moriano-Gutierrez et al., 2019; Wier et al., 2010). How host communication is mediated to drive development and maturation of these networks is currently unknown. In this study, we used NanoSIMS to trace stable isotope-labelled bacterial products in host tissues during initial interactions of *V. fischeri* with *E. scolopes*. Our data show that light-organ tissues are unique in this animal in being highly permissive to biomolecule uptake. The specificity of host response is mediated by differences in mechanisms of molecular transfer that occur across the biogeography of the organ.

2 | RESULTS

2.1 | The nascent light-organ epithelia comprise the most susceptible host tissues to uptake biomolecules from *V. fischeri*

Upon a 2- or 3.5-hr exposure to ^{15}N-enriched *V. fischeri* ES114 cells, when the cells had associated with the surface but had not yet colonised the tissues, all epithelial regions of the light organ became labelled in ^{15}N (Figure 2a and Table S1). The superficial areas of the light organ (i.e., ciliated fields and pores), where *V. fischeri* cells aggregate and enter host tissues, and the deeper long-term residence of *V. fischeri* (the crypts) were most strongly labelled. In contrast, the portions of the migration pathway from pore to crypts, that is, the ducts/antechambers, were not as vividly labelled. These data suggest that susceptibility of the cells to incorporation of exported *V. fischeri* molecules was more important for labelling pattern than diffusion time or distance. Within the host cells, ^{15}N labelling (Figure 2b) of bacterial products was detectable in two regions: the nucleolus, where it was most pronounced, and the euchromatin (Figure 2c,d and Table S1).

^{15}N-labelled biomolecules of *V. fischeri* cells were also occasionally detected in a few nonepithelial cells of the light organ, including in (a) the haemocytes of the blood sinuses that support the superficial ciliated fields (Figures 1b and 3a and Table S2); (b) the cells of the reflector, which lies dorsal to the crypts to reflect bioluminescent light ventrally (Figures 1c and 3b and Table S2); and (c) the connective tissue cells that support the crypts (Figures 1c and 3c and Table S2). Labelling also occurred occasionally in the cells of other tissues but was only statistically significantly different from background in epithelial or endothelial tissues (Figure 3d–g and Table S2). When labelling was detected, the patterns were similar to those noted in the light-organ epithelia, that is, in the nucleolus and euchromatin.

2.2 | The host uptake of ^{15}N-labelled biomolecules was not specific to products of *V. fischeri*

We also exposed juvenile squids to strongly ^{15}N-enriched nonsymbiotic Vibrionaceae cells, *Vibrio campbellii* KNH1 and *Photobacterium*
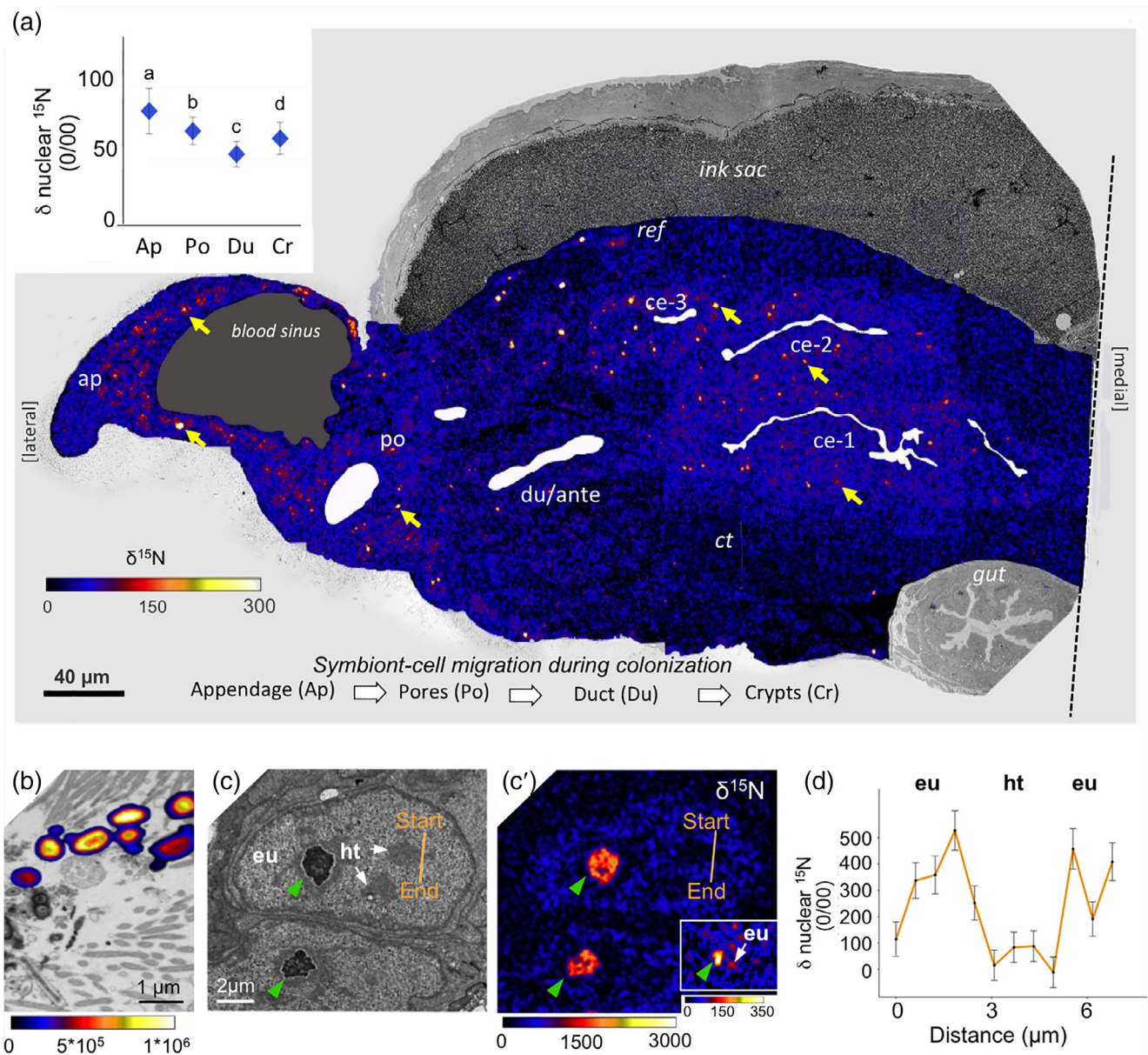
FIGURE 2 Uptake of isotope-labelled *Vibrio fischeri* products into light-organ epithelial cells of a juvenile host. (a) ^{15}N enrichment (expressed as δ^{15}N) in the light organ of a newly hatched animal at 2 hr postexposure to 10^6 intact ^{15}N-labelled *V. fischeri* cells ml^{-1} of seawater; the data were obtained from all nuclei in the mosaic, independent of enrichment level. A composite transmission electron microscopy micrograph and the corresponding mosaic of 65 individual, high-resolution nanoscale secondary ion mass spectrometry (NanoSIMS) images. Labelling was abundant and appeared as hotspots in the nucleoli of all light-organ epithelia (e.g., yellow arrows) with which *V. fischeri* cells interface, that is, the surface ciliated field, here showing the epithelia of the anterior appendage (ap), the pore (po), the duct/antechamber (du/ante), and crypts (crypt epithelia, ce-1–3); *ct*, connective tissue; *ref*, reflector. Inset, upper left, the average level of ^{15}N enrichment in cell nuclei in different epithelial regions. Data were derived from the mosaic (Ap, n = 56; Po, n = 58; Du, n = 36; Cr, n = 142). Lowercase letters indicate statistically significant differences between the light-organ compartments (Kruskal–Wallis test with Nemenyi post hoc, P < .0001). Error bars represent 1 standard deviation. (b) ^{15}N-labelled *V. fischeri* cells migrating through the ducts. (c, c′) Transmission electron microscopy (left) and NanoSIMS (right) images of two cells of the crypt epithelium, defining the region scanned (start–end) for ^{15}N/^{14}N ratio within the nucleus, showing strong enrichment in the nucleoli (green arrows) and euchromatin (eu); ht, heterochromatin. (c′) NanoSIMS at two sensitivities (main, lower, and inset higher sensitivity, respectively) to highlight less intense labelling of the chromatin. (d) A representative image of the quantification of ^{15}N enrichment through the region scanned in (c). Points are averages of NanoSIMS scans (n = 10) ± 1 standard deviation

leiognathi KHN6, which are, in comparison with *V. fischeri*, rare phylotypes in the host's environment (Jones, Maruyama, Ouverney, & Nishiguchi, 2007). These experiments were done with a 3-hr exposure to labelled cells, a period when, in the absence of *V. fischeri* in the environment, these strains exhibit aggregation on the light-organ surface indistinguishable from that of the nascent symbiont (Koehler et al.,
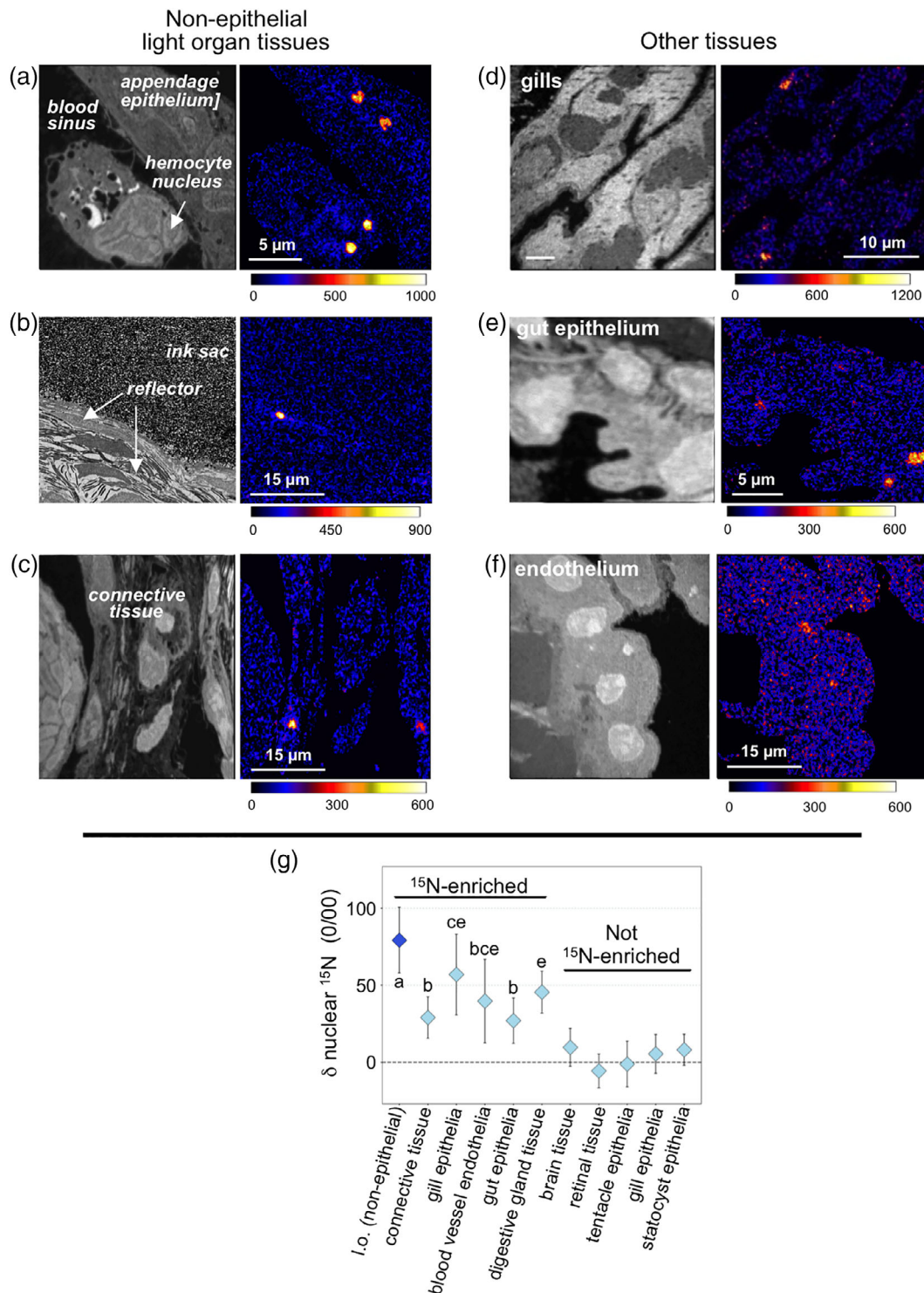
FIGURE 3 The ^{15}N enrichments in tissues not directly associating with the symbiont. Nuclei and nucleoli (hotspots) in (a–c) light organ nonepithelial tissues and in (d–f) epithelial tissues in other squid organs after 3.5 hr of inoculation with ^{15}N-labelled *Vibrio fischeri* cells. Left panels show tissue structure (nanoscale secondary ion mass spectrometry $^{12}C^{14}N^{-}$ image). Right panels show corresponding, quantified nanoscale secondary ion mass spectrometry $^{15}N/^{14}N$ ratio image. (g) Representative ^{15}N enrichments in nuclei of a single animal (excluding the nucleolus when visible) in different tissues across the body. Nonepithelial tissue inside the light organ (l.o.; n = 72), connective tissue (n = 59), and tissues outside of the light organ: gill epithelia (n = 34), blood vessel endothelial cells (n = 48), gut epithelia (n = 100), digestive gland cells (n = 31), brain (n = 16), retina (r; n = 11), tentacles (n = 29), white body (n = 27), and epithelium supporting statolith (n = 27). Only enriched tissues were considered in the statistical analysis. Lowercase letters indicate statistically significant differences between the different tissues (Kruskal–Wallis test with Nemenyi post hoc, P < .0001). Points are averages ± 1 standard deviation. Dashed line, limit of detection, or no difference between the control value for the natural distribution of ^{15}N over ^{14}N in the sample
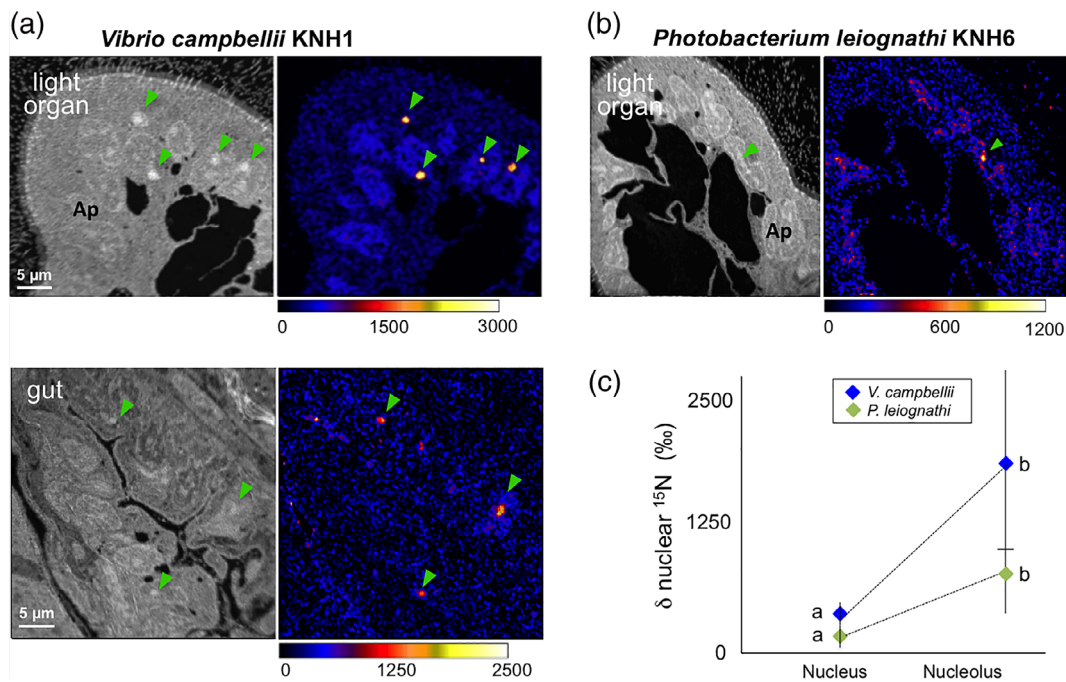
FIGURE 4 ^{15}N enrichment (δ^{15}N) in juvenile tissues with ^{15}N-labelled nonsymbiotic Vibrionaceae cells. Animals were analysed at 3.5 hr postinoculation. (a, b) Left panels, tissue structure (nanoscale secondary ion mass spectrometry $^{12}C^{14}N^{-}$ image); right panels, corresponding quantified image of nanoscale secondary ion mass spectrometry $^{15}N/^{14}N$ ratio; nucleoli, green arrows. Ap, anterior appendage of the light organ. (c) Average ^{15}N enrichment in the nucleus ($n = 236$, *Vibrio campbellii*; $n = 196$, *Photobacterium leiognathi*) and nucleolus ($n = 73$, *V. campbellii*; $n = 57$, *P. leiognathi*) of the light-organ surface epithelium from 5–7 individual animals. Points are average ± 1 standard deviation. Lowercase letters indicate statistically significant differences between the light-organ compartments (Kruskal–Wallis test with Nemenyi post hoc, $P < .0001$)

2018). Under these conditions, these strains produced ^{15}N-enrichment patterns in the light organ similar to those induced by *V. fischeri* cells (Figure 4 and Table S3).

The enrichment in the crypts with the brief 3-hr exposure to *V. fischeri* cells, which have not yet moved into host tissues, and the nonsymbiotic strains, which do not colonise, suggested that labelling of the crypt cells was not the result of direct interaction with bacterial cells but rather through uptake of materials exported from the bacteria and conveyance along the short path to the crypts. Other studies of the squid–vibrio system demonstrated that OMVs presented by *V. fischeri* in the crypt spaces drive symbiont-induced host morphogenesis (Aschtgen, Lynch, et al., 2016; Aschtgen, Wetzel, et al., 2016). Further, purified OMVs of *V. fischeri* mimicked the morphogenic influence of intact *V. fischeri* cells and, although other bacterial cells do not colonise the host crypt spaces, their isolated OMVs also induce morphogenesis. Thus, we first determined whether stable-isotope enrichment of host light-organ cells occurred in response to OMVs derived from ^{15}N-labelled *V. fischeri* ES114. The enrichment in light-organ tissues with symbiont OMVs was similar to that of symbiont cells, although the response to OMVs potentially occurred more quickly (Figure 5a and Table S4). To compare with other bacteria phylotypes, we chose OMVs derived from the closely related *V. campbelli* KNH1 and the more distantly related *Escherichia coli* RP437. Substantial, statistically significant differences in enrichment were observed among the different bacterial species, with host cells most enriched for OMV-derived molecules from *V. campbellii* and least from those of *E. coli* (Figures 5b,c and S1 and Table S5). Further, enrichment with OMVs localized to similar areas of the host cells as intact bacteria.

Finally, to determine how general the phenomenon of light-organ permissiveness might be, we exposed squid to a mixture of ^{15}N-enriched amino acids. Similar to the natural dissolved organic material (DOM) uptake by marine invertebrate tissues (Gomme, 2001; Stephens, 1988; Wright & Manahan, 1989), these labelled amino acids were taken up by host cells of the light organ and had similar subcellular enrichment patterns as intact bacteria and OMVs, suggesting that the majority of bacterial molecules were transferred to the host as part of a more general transfer mechanism from the environment (Table S6).

Taken together, these data provide evidence that, under these experimental conditions, biomolecules shed from intact bacterial cells, OMVs, or other biomolecules from the environment move through the migratory pathway of the squid light organ from pore to crypts, and are taken up by superficial and crypt epithelial cells, and that nitrogen from these molecules is incorporated into the nucleus. Specificity in the response in the crypts to *V. fischeri* materials occurs because, under natural conditions, only the symbiont can enter and grow in the crypts to present high concentrations of OMVs or other biomolecules.

3 | DISCUSSION

The isotopic labelling strategy, in combination with correlated transmission electron microscopy (TEM) and NanoSIMS imaging, revealed a high level of transfer of ^{15}N-containing molecular compounds from environmental bacteria and their OMVs to the juvenile squid light-organ tissues and to a lesser degree other epithelial tissues.

3.1 | Insights into host–symbiont communication from NanoSIMS studies

By integrating the information gained in these NanoSIMS analyses with previous work on the squid–vibrio model, the results of this study demonstrate that (a) the symbiotic organ of the juvenile animal, in comparison with other regions of the body, is highly permissive to the uptake of environmental biomolecules; (b) the specificity of

response during initial symbiont recruitment from the bacterioplankton is the result of presentation of products exclusive to *V. fischeri*; (c) specificity of certain host responses following of the crypts is, at least in part, the result of the presentation of high levels of evolutionarily conserved bacterial cargo, notably MAMPs and OMVs, in host regions restricted to by *V. fischeri*; (d) biomolecules traffic strongly to the nucleus in this animal, as they do in mammalian cells, particularly the euchromatin and nucleolus; and (e) NanoSIMS is a valuable tool for the study of host–symbiont dynamics.

It was not surprising to find uptake of environmental N-containing molecules by squid tissues: The body plan of molluscs, such as squid, is comparatively open; that is, the organs are continually exposed to bacteria-rich water (~10^6 cells ml^{-1} of seawater) through the ventilation of the mantle/body cavity (Figure 1a). Unlike terrestrial animals, which internalised their mucus membranes during the water-to-land transition, the squid and other soft-bodied marine invertebrates expose their mucus membranes directly to the aqueous environment. With such a tissue arrangement, these animals have the shared-derived character of using DOMs as a nutrient source. This capability also means that they must prevent uncontrolled "fouling" of their body surfaces by growth of the abundant microbes in the water, not only to dissuade microbial overgrowth of their tissue surfaces but also to stem competition with microbes for limited DOM.

How might some responses of the host to imported molecules be specific to *V. fischeri* cells? The light-organ surface epithelia were strongly enriched in ^{15}N produced by either the specific symbiont or nonsymbiotic bacteria. Because, within the first 2–3 hr, the host discriminates between the thousands of nonsymbiotic bacteria in seawater
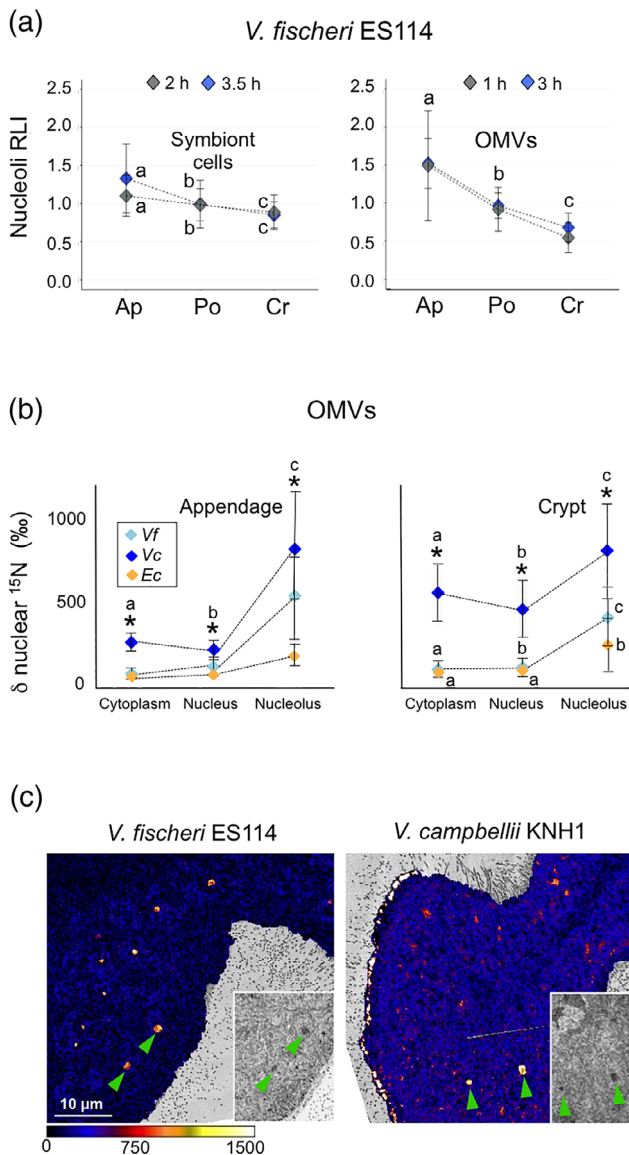

FIGURE 5 ^{15}N enrichment of light-organ regions upon exposure to outer membrane vesicles (OMVs). (a) Relative labelling index (RLI) for ^{15}N enrichment in light organs exposed for different time periods. Left, to intact *Vibrio fischeri* cells for 2 hr (*n* = 3) or 3.5 hr (*n* = 6); 6–10 nucleoli per region for each animal; right, to purified OMVs for 1 hr (*n* = 5) or 3 hr (*n* = 4). Ap, anterior appendage (cells: *n* = 37, 2 hr; *n* = 90, 3.5 hr; OMVs: *n* = 44, 1 hr; *n* = 48, 3 hr); Po, pore (cells: *n* = 44, 2 hr; *n* = 54, 3.5 hr; OMVS: *n* = 55, 1 hr; *n* = 42, 3 hr); Cr, crypt (cells: *n* = 80, 2 hr; *n* = 73, 3.5 hr; OMVs: *n* = 65, 1 hr; *n* = 44, 3 hr). Points are averages ± 1 standard deviation. Lowercase letters indicate statistically significant differences between the light-organ compartments (two-way analysis of variance with Tukey post hoc, *P* < .0001). (b) Quantification of the distribution of ^{15}N enrichment in subcellular regions of the anterior appendage and crypt in animals exposed to the OMVs of *V. fischeri* (*n* = 3), *Vibrio campbellii* (*n* = 5), and *Escherichia coli* (*n* = 3). For each animal, cytoplasm *n* = 31–64; nucleus *n* = 101–373; and nucleolus *n* = 829–868. Points are averages ± 1 standard deviation. Lowercase letters indicate significant differences between the cell organelles (Kruskal–Wallis test with Nemenyi post hoc, *P* < .0001); asterisks indicate significant differences between bacteria species (Kruskal–Wallis test, *P* < .0001). (c) A comparison of ^{15}N enrichment in epithelium of the superficial anterior appendage of the light organ between animals exposed to labelled OMVs from *V. fischeri* or *V. campbellii*. Images of nanoscale secondary ion mass spectrometry ^{15}N/^{14}N ratios; inset, corresponding mosaic transmission electron microscopy micrographs; nucleoli, green arrows

and its coevolved symbiont, *V. fischeri*, the high general permissiveness of the organ to environmental biomolecules was unexpected. An earlier study of the system had shown that, even in the background of the typical ~10^6 nonspecific bacteria per ml of seawater, the entire light organ responds with changes in its transcriptome only with the attachment and aggregation on the ciliated surface of as few as 5–10 *V. fischeri* cells (Kremer et al., 2013). In this earlier study, the insensitivity to nonspecific bacteria was underscored by the finding that no difference in the transcriptomic response was detected in (a) aposymbiotic animals, that is, those exposed to natural, microbe-rich, seawater with no *V. fischeri* present, and (b) animals that were maintained entirely axenic for the same period. Our data, including the observation that squids exposed to an artificial mixture of ^{15}N-enriched amino acids showed comparable cellular ^{15}N-distributions, suggest that the majority of bacterial molecules are transferred to the host as part of a more general material conveyance from the environment. It is likely that the host ^{15}N-enrichment patterns that were shared between all treatments are guided by similar signalling pathways within the host cells. On the other hand, substantial differences in the host's ^{15}N enrichment were observed when squids where exposed to OMVs derived from different bacteria; specifically, *V. fischeri*, *V. campbellii*, and *E. coli* (Figures 5 and S1). These "OMV ^{15}N-enrichment patterns" were distinct, especially between the two *Vibrio* species and *E. coli*, demonstrating the host's preference for specific uptake of molecules derived from different bacteria. Together, these data indicate that *V. fischeri*, the only bacterium that can colonise the crypts, delivers cargo to which the animal responds with extremely high specificity; that is, an exclusive host–symbiont dialogue is in play.

The other highly permissive regions of the organ were the crypt spaces. Unlike the surface, where specificity of the response must be mediated by *V. fischeri*-specific biochemistry, the crypts respond to *V. fischeri* MAMPs, notably lipopolysaccharide and peptidoglycan derivatives, and OMVs (Aschtgen, Lynch, et al., 2016; Aschtgen, Wetzel, et al., 2016; Koropatnick et al., 2004). MAMPs and OMVs isolated from other Gram-negative bacteria, which freely diffuse into the light-organ crypts, induce host development similar to the *V. fischeri* cells that populate the crypt spaces. Thus, the specificity of the crypt response is the result of the restriction of this space to the symbiont cells. Once the signalling from the crypts induces development, the ciliated surfaces regress through apoptosis of its cells over a few days. The light-organ permissiveness of molecular uptake is then exclusive to the crypt epithelia, likely throughout the nearly year-long lifetime of the host and its symbiotic association with *V. fischeri*.

Although the induction of the dramatic morphogenesis of the light-organ surface is relatively well characterized as MAMPs signalling through the crypt epithelia, other aspects of light-organ development and maturation are not. For example, upon, the bottleneck leading to the crypt narrows, ensuring that *V. fischeri* cells are limited to that region, that is, except during venting, they are not typically abundant in the ducts or antechambers (Figures 1b and 2a). In addition, we do not know the mechanisms underlying the symbiosis-induced change in gene expression in remote tissues. Likely, the observed ^{15}N enrichment reflects transport and trafficking of other bioactive symbiont molecules.

Promising candidates include proteins in the OMVs. A study of 49 *Helicobacter pylori* proteins with a nuclear localization signal showed that almost half did traffic to the nucleus (Lee, Jun, Kim, Baik, & Lee, 2015). The *V. fischeri* OMV proteome has over 200 proteins (Lynch et al., 2019), and three of the proteins have a nuclear localization signal in all of the 13 symbiotic *V. fischeri* strains that have a full-genome sequence. Two of the three, FadJ and PslD (involved in fatty acid metabolism and polysaccharide export, respectively), are encoded by non-essential genes carried in the OMVs of bacterial pathogens (Choi et al., 2011; Lee et al., 2012; Lee et al., 2017); the gene for one of the three, *fadJ*, encodes a nuclear localization signal in *Klebsiella pneumonia*. In addition to proteins, DNA (Berleman & Auer, 2013) and RNA (Habier et al., 2018) are attractive candidates as *V. fischeri* OMV molecules transported to the squid-host nucleus. For example, in a recent paper, DNA from OMVs of *Pseudomonas aeruginosa* was detectable in host nuclear fraction (Bitto et al., 2017).

In all cases, the most abundant trafficking of ^{15}N-enriched biomolecules within the squid animal cells was to the nucleus, particularly strongly to the euchromatin, sites of active transcription, and the nucleolus, the protein-rich nuclear feature where ribosome biogenesis occurs. Recent studies have indicated that the nucleolus is multifunctional, with roles in gene stability and silencing, cell-cycle regulation, stress, and immune response (Boisvert, van Koningsbruggen, Navascues, & Lamond, 2007; Grummt, 2013). For example, recent NanoSIMS analyses have shown that cancer drugs, which influence these sorts of activities in the cell, showed strong stable-isotope labelling in the nucleolus (Lee et al., 2017; Lee et al., 2017). Further, all processes of the above-mentioned functions of the nucleolus are ones that are influenced by interactions with microbes. In some infections with intracellular (Bierne, 2013) and extracellular pathogens (Dean et al., 2010; Holmes, Muhlen, Roe, & Dean, 2010), exported products localize to the nucleolus or influence nucleolar function. It should be noted that, although nucleus and nucleoli label strongly in NanoSIMS experiments in a number of circumstances (Takado et al., 2015), such localization is not always the case. In a recent study tracing materials exported from the coral pathogen, *Vibrio coralliilyticus*, ^{15}N enrichment localized to secretory vesicles in the cells of the host coral (Gibbin et al., 2019).

3.2 | The pros and cons of using NanoSIMS for the study of symbiotic systems

The power of NanoSIMS correlated with TEM lies in the resulting high resolution of biomolecular signatures (for review, see Jiang, Kilburn, Decelle, & Musat, 2016). Fluorescence microscopy is limited to visualisation by light microscopy. Further, unlike observation of biological structures by fluorescence, stable isotope labelling detection has low impact on molecular size, structure, and biological function. A major drawback of NanoSIMS/TEM is the cost of the associated equipment, which restricts its availability to dedicated facilities. In addition, tissue analyses, such as those presented in this contribution, are time consuming; as such, analyses are limited to low sample number. Additionally, in studies such as ours, it can be difficult to track exactly which molecules

are being detected, which can be overcome by complementing these analyses with other techniques. These challenges notwithstanding, isotope labelling with the high resolution of NanoSIMS/TEM has provided biologists with a powerful method by which to characterize the interactions between microbes and their animal or plant hosts (Musat, Musat, Weber, & Pett-Ridge, 2016). Most of these studies have focused on nutrient transfer and metabolic processes (for review, see Berry & Loy, 2018). For example, in characterization of symbiont to host transfer of biomolecules, NanoSIMS has been used to (a) localize ^{15}N-labelled nitrogen-fixing bacteria inside of coral larvae (Lema et al., 2016); (b) visualise the transfer of fixed nitrogen molecules from the bacteria symbionts to the marine shipworm and cockroach hosts (Tai et al., 2016; Volland et al., 2018); (c) trace the incorporation of labelled C- and N-containing photosynthates translocated from symbiotic algae to their coral host (Kopp et al., 2013; Kopp et al., 2015); and (d) describe the nutritional interaction between the coral host and its symbiont under pathogenic conditions (Gibbin et al., 2019). In addition, several studies have examined transfer of molecules from the host to its symbionts. For example, NanoSIMS revealed that newly photoassimilated C and N from plant roots supports the nutrient demands of their associated soil microbes (Kaiser et al., 2015). In studies of mammals, fluorescent in situ hybridization and NanoSIMS were combined to characterize usage of host proteins by gut microbes; the intestinal microbial population was observed to forage on host-derived labelled proteins that were secreted into the mucin (Berry et al., 2013). The studies of the squid–vibrio system reported here highlight a novel use of NanoSIMS to study the microbiogeographical patterns of host–symbiont interaction during symbiosis onset.

4 | EXPERIMENTAL PROCEDURES

4.1 | General procedures

Adult *E. scolopes* were collected on Oahu, Hawai'i, and transported to the Kewalo Marine Laboratory, where breeding animals were maintained in a flow-through seawater system (for review, see McFall-Ngai, 2014b). For methods associated with NanoSIMS analyses, see the Supporting Information.

4.2 | Ethics statement

The animal host was maintained in seawater facilities at University of Hawai'i at Mānoa. All experiments were performed in accordance with the relevant regulatory standards established by the University of Hawai'i at Mānoa.

4.3 | Bacterial species and growth conditions

Strains of four bacteria species were used in this study: wild-type *V. fischeri* ES114 (Boettcher & Ruby, 1990), *V. campbellii* KNH1

(formerly, *Vibrio parahaemolyticus* KNH1; Nyholm, Stabb, Ruby, & McFall-Ngai, 2000), *Photobacterium leognathi* KNH6 (Koehler et al., 2018), and *E. coli* RP437 (Zhou, White, Polissi, Georgopoulos, & Raetz, 1998). The *Vibrio* spp. and *P. leognathi* were grown overnight on LBS agar plates (Luria broth agar containing an additional 2% [wt/vol] NaCl; Graf, Dunlap, & Ruby, 1994); *E. coli* was cultured in Luria broth medium (Bertani, 1951). One colony of bacteria cells was then transferred to a minimal salts media (Ruby & Nealson, 1977), which was supplemented with 11 mM of [^{15}N]-ammonium chloride (NH$_4$Cl; ^{15}N, 99%; Cambridge Isotope Laboratories, Inc., MA, USA), 40 mM of glycerol, 50 mM of PIPES buffer (pH 7.2), and 5 g L^{-1} of Celtone base powder (^{15}N, 98%; Cambridge Isotope Laboratories, Inc., MA, USA). Cultures of 100 ml were grown shaking at 28°C. Levels of ^{15}N enrichment were maximised by a serial subculturing of the bacteria into fresh labelled media (initial OD$_{600\,nm}$ of 0.0025, i.e., 30–40 generations). Cells from the last passage (OD$_{600\,nm}$ of 0.2–0.5) were thoroughly washed twice in filtered seawater (0.2-μm Millipore membrane) by centrifugation (2 min, 8,000 rpm) immediately before inoculating the squid. NanoSIMS control samples containing the natural ^{15}N/^{14}N isotopic composition analysis were derived following the same protocol, except that bacteria were grown in nonlabelled medium. In addition, we tested whether carryover from labelled cells into the seawater where the squid were inoculated would confound the conclusions of the results (see the Supporting Information). No confounding effect was detected in these experiments.

4.4 | OMV purification and preparation for TEM and NanoSIMS

OMVs were purified from heavy-isotope-labelled bacteria using a method adapted from Aschtgen, Wetzel, et al. (2016). Purified OMVs were visualised with TEM either by negative staining or ultrathin sections of embedded samples. For negative staining, samples were applied to 400-mesh carbon-coated copper grids, stained with 2% uranyl acetate, washed, dried, and analysed by TEM. OMVs were viewed by NanoSIMS by the same methods used for analysis of exposure to whole bacteria.

4.5 | Exposure of animals to labelled materials and preparation for NanoSIMS

Following hatching, juvenile *E. scolopes* were placed in filter-sterilised instant ocean that contained ^{15}N-labelled bacterial cells, ^{15}N-labelled purified OMVs, or ^{15}N-labelled free amino acids. To determine how bacterial compounds interact with squid cells in early-stage symbiosis, individual animals were placed in glass vials with labelled cells at 10^6 cfu ml^{-1} of seawater for 2 hr (n = 3), whereas animals exposed under these conditions to labelled OMVs for 1 or 3 hr (n = 4–5, respectively). For all of the bacterial strains used, the juvenile squid were exposed to higher inocula than the average number of these

species in Hawaiian near-shore habitats (for numbers of planktonic *V. fischeri* strains, see (Ruby & Lee, 1998); *V. campbellii* and *P. leiognathi*, see (Jones et al., 2007); and *E. coli*, see Cui, Yang, Pagaling, & Yan, 2013). However, 10^6 cells ml^{-1} does represent the typical number of total bacteria of all Gram-positive and Gram-negative species in near-shore Hawaiian waters, with Gammaproteobacteria species at ~10^5 cells ml^{-1} (Jones et al., 2007). Earlier work on the system showed that an increase in inoculum size results in larger numbers of bacteria in the aggregates but does not change the numbers of *V. fischeri* that enter each crypt space, which averages one or two cells (Wollenberg & Ruby, 2009) that grow out to ~10^5–10^6 to fill the juvenile crypt spaces.

Animals were prepared for TEM as previously described (Heath-Heckman et al., 2016). From blocks of animal samples embedded for TEM, semithin and ultrathin sections (about 0.5 µm and about 70 nm, respectively) were cut and semithin sections were stained with toluidine blue–borax and imaged with a light microscope Leica DMRB equipped with AxioCam MRc5 camera (Zeiss, Germany) to aid in visually navigating the squid tissues. Sections for NanoSIMS analysis were prepared in two different ways: (a) high-resolution imaging for correlative TEM and NanoSIMS. Ultrathin sections (about 70 nm) were mounted on either formvar-coated alpha numeric grids (200 mesh) or oval slot grids with polystyrene film. Grids were then counterstained with 4% uranyl acetate and Reynolds lead citrate, then observed at 80 kV with a TEM Philips CM100. Prior to the NanoSIMS imaging of the slot-grid samples, small holes defining the area of interest were punched in the section using the electron beam to mark the corners of the area to aid in navigating the sample. Subsequently, the polystyrene film with the section was carefully separated from the grid and mounted on a 10-mm coverslip. This procedure allowed for better stability of the section under the NanoSIMS ion beam. (b) For large-area coverage for statistical analyses (Figure 2a). Semithin sections (0.5 µm) were mounted on 10-mm coverslips and stained with toluidine blue–borax (pH 9.5).

4.6 | Statistical analyses

Differences in relative labelling index between the light-organ compartments (appendage, pore, and crypt) at both time points were tested using a two-way factorial analysis of variance test after log transformations of the data followed by the Tukey honestly significant difference test for multigroup comparison. When the data did not meet the assumptions of the parametric test, significance of ^{15}N enrichment levels among cell organelles and bacteria strains was assessed using the nonparametric Kruskal–Wallis ranked test followed by a Nemenyi post hoc test. Correlations between the levels of ^{15}N enrichment in the nucleus and nucleolus were examined using the nonparametric Spearman's rank correlation. All statistical analyses were performed using the statistical program R (Maxwell & Delaney, 2004), Version 3.2.0. Data are expressed as means ± standard deviation. *P* values of <.05 were considered as statistically significant for all testing.

CONFLICT OF INTEREST

The authors declare no conflicts of interest.

ORCID

Margaret McFall-Ngai https://orcid.org/0000-0002-6046-6238

REFERENCES

Altura, M. A., Heath-Heckman, E. A., Gillette, A., Kremer, N., Krachler, A. M., Brennan, C., … McFall-Ngai, M. J. (2013). The first engagement of partners in the *Euprymna scolopes–Vibrio fischeri* symbiosis is a two-step process initiated by a few environmental symbiont cells. *Environmental Microbiology*, 15, 2937–2950. https://doi.org/10.1111/1462-2920.12179

Aschtgen, M. S., Lynch, J. B., Koch, E., Schwartzman, J., McFall-Ngai, M., & Ruby, E. (2016). Rotation of *Vibrio fischeri* flagella produces outer membrane vesicles that induce host development. *Journal of Bacteriology*, 198, 2156–2165. https://doi.org/10.1128/JB.00101-16

Aschtgen, M. S., Wetzel, K., Goldman, W., McFall-Ngai, M., & Ruby, E. (2016). *Vibrio fischeri*-derived outer membrane vesicles trigger host development. *Cellular Microbiology*, 18, 488–499. https://doi.org/10.1111/cmi.12525

Berleman, J., & Auer, M. (2013). The role of bacterial outer membrane vesicles for intra- and interspecies delivery. *Environmental Microbiology*, 15, 347–354. https://doi.org/10.1111/1462-2920.12048

Berry, D., & Loy, A. (2018). Stable-isotope probing of human and animal microbiome function. *Trends in Microbiology*, 26, 999–1007. https://doi.org/10.1016/j.tim.2018.06.004

Berry, D., Stecher, B., Schintlmeister, A., Reichert, J., Brugiroux, S., Wild, B., … Wagner, M. (2013). Host-compound foraging by intestinal microbiota revealed by single-cell stable isotope probing. *Proceedings of the National Academy of Sciences U S A*, 110, 4720–4725. https://doi.org/10.1073/pnas.1219247110

Bertani, G. (1951). A method for detection of mutations, using streptomycin dependence in *Escherichia coli*. *Genetics*, 36, 598–611.

Bierne, H. (2013). Nuclear microbiology—Bacterial assault on the nucleolus. *EMBO Reports*, 14, 663–664. https://doi.org/10.1038/embor.2013.105

Bitto, N. J., Chapman, R., Pidot, S., Costin, A., Lo, C., Choi, J., … Ferrero, R. L. (2017). Bacterial membrane vesicles transport their DNA cargo into host cells. *Scientific Reports*, 7, 7072. https://doi.org/10.1038/s41598-017-07288-4

Boettcher, K. J., & Ruby, E. G. (1990). Depressed light emission by symbiotic *Vibrio fischeri* of the sepiolid squid *Euprymna scolopes*. *Journal of*

Bacteriology, *172*, 3701–3706. https://doi.org/10.1128/jb.172.7.3701-3706.1990

Boisvert, F. M., van Koningsbruggen, S., Navascues, J., & Lamond, A. I. (2007). The multifunctional nucleolus. *Nature Reviews Molecular and Cell Biology*, *8*, 574–585. https://doi.org/10.1038/nrm2184

Bongrand, C., & Ruby, E. G. (2018). Achieving a multi-strain symbiosis: Strain behavior and infection dynamics. *ISME Journal*, *13*, 698–706. https://doi.org/10.1038/s41396-018-0305-8

Bright, M., & Bulgheresi, S. (2010). A complex journey: Transmission of microbial symbionts. *Nature Reviews Microbiology*, *8*, 218–230. https://doi.org/10.1038/nrmicro2262

Choi, D. S., Kim, D. K., Choi, S. J., Lee, J., Choi, J. P., Rho, S., ... Gho, Y. S. (2011). Proteomic analysis of outer membrane vesicles derived from *Pseudomonas aeruginosa*. *Proteomics*, *11*, 3424–3429. https://doi.org/10.1002/pmic.201000212

Chun, C. K., Troll, J. V., Koroleva, I., Brown, B., Manzella, L., Snir, E., ... McFall-Ngai, M. J. (2008). Effects of colonization, luminescence, and autoinducer on host transcription during development of the squid–vibrio association. *Proceedings of the National Academy of Sciences USA*, *105*, 11323–11328. https://doi.org/10.1073/pnas.0802369105

Cossart, P. (2000). *Cellular microbiology*. Washington, DC: ASM Press.

Cossart, P. (2018). *The new microbiology: From microbiomes to CRISPR* (Washington, DC: ASM Press,), pp. 1 online resource.

Cui, H., Yang, K., Pagaling, E., & Yan, T. (2013). Spatial and temporal variation in enterococcal abundance and its relationship to the microbial community in Hawaii beach sand and water. *Applied and Environmental Microbiology*, *79*, 3601–3609. https://doi.org/10.1128/AEM.00135-13

Dean, P., Scott, J. A., Knox, A. A., Quitard, S., Watkins, N. J., & Kenny, B. (2010). The enteropathogenic *E. coli* effector EspF targets and disrupts the nucleolus by a process regulated by mitochondrial dysfunction. *PLoS Pathogens*, *6*, e1000961. https://doi.org/10.1371/journal.ppat.1000961

Donaldson, G. P., Lee, S. M., & Mazmanian, S. K. (2016). Gut biogeography of the bacterial microbiota. *Nature Reviews Microbiology*, *14*, 20–32. https://doi.org/10.1038/nrmicro3552

Gibbin, E., Gavish, A., Krueger, T., Kramarsky-Winter, E., Shapiro, O., Guiet, R., ... Meibom, A. (2019). *Vibrio coralliilyticus* infection triggers a behavioural response and perturbs nutritional exchange and tissue integrity in a symbiotic coral. *ISME Journal*, *13*, 989–1003. https://doi.org/10.1038/s41396-018-0327-2

Gomme, J. (2001). Transport of exogenous organic substances by invertebrate integuments: The field revisited. *Journal of Experimental Zoology*, *289*, 254–265.

Graf, J., Dunlap, P. V., & Ruby, E. G. (1994). Effect of transposon-induced motility mutations on colonization of the host light organ by *Vibrio fischeri*. *Journal of Bacteriology*, *176*, 6986–6991. https://doi.org/10.1128/jb.176.22.6986-6991.1994

Graf, J., & Ruby, E. G. (1998). Host-derived amino acids support the proliferation of symbiotic bacteria. *Proceedings of the National Academy of Sciences U S A*, *95*, 1818–1822. https://doi.org/10.1073/pnas.95.4.1818

Grummt, I. (2013). The nucleolus—Guardian of cellular homeostasis and genome integrity. *Chromosoma*, *122*, 487–497. https://doi.org/10.1007/s00412-013-0430-0

Habier, J., May, P., Heintz-Buschart, A., Ghosal, A., Wienecke-Baldacchino, A. K., Nolte-'t Hoen, E. N. M., ... Fritz, J. V. (2018). Extraction and analysis of RNA isolated from pure bacteria-derived outer membrane vesicles. *Methods in Molecular Biology*, *1737*, 213–230. https://doi.org/10.1007/978-1-4939-7634-8_13

Holmes, A., Muhlen, S., Roe, A. J., & Dean, P. (2010). The EspF effector, a bacterial pathogen's Swiss army knife. *Infection and Immunity*, *78*, 4445–4453. https://doi.org/10.1128/IAI.00635-10

Jiang, H., Kilburn, M. R., Decelle, J., & Musat, N. (2016). NanoSIMS chemical imaging combined with correlative microscopy for biological sample analysis. *Current Opinion in Biotechnology*, *41*, 130–135. https://doi.org/10.1016/j.copbio.2016.06.006

Jones, B. W., Maruyama, A., Ouverney, C. C., & Nishiguchi, M. K. (2007). Spatial and temporal distribution of the Vibrionaceae in coastal waters of Hawaii, Australia, and France. *Microbial Ecology*, *54*, 314–323. https://doi.org/10.1007/s00248-006-9204-z

Kaiser, C., Kilburn, M. R., Clode, P. L., Fuchslueger, L., Koranda, M., Cliff, J. B., ... Murphy, D. V. (2015). Exploring the transfer of recent plant photosynthates to soil microbes: Mycorrhizal pathway vs direct root exudation. *New Phytologist*, *205*, 1537–1551. https://doi.org/10.1111/nph.13138

Koehler, S., Gaedeke, R., Thompson, C., Bongrand, C., Visick, K. L., Ruby, E., & McFall-Ngai, M. (2018). The model squid–vibrio symbiosis provides a window into the impact of strain- and species-level differences during the initial stages of symbiont engagement. *Environmental Microbiology*, *21*, 3269–3283. https://doi.org/10.1111/1462-2920.14392

Kopp, C., Domart-Coulon, I., Escrig, S., Humbel, B.M., Hignette, M., & Meibom, A. (2015). Subcellular investigation of photosynthesis-driven carbon assimilation in the symbiotic reef coral *Pocillopora damicornis*. *mBio*, *6*, doi: https://doi.org/10.1128/mBio.02299-14

Kopp, C., Pernice, M., Domart-Coulon, I., Djediat, C., Spangenberg, J. E., Alexander, D. T., ... Meibom, A. (2013). Highly dynamic cellular-level response of symbiotic coral to a sudden increase in environmental nitrogen. *mBio*, *4*, e00052–e00013. https://doi.org/10.1128/mBio.00052-13

Koropatnick, T. A., Engle, J. T., Apicella, M. A., Stabb, E. V., Goldman, W. E., & McFall-Ngai, M. J. (2004). Microbial factor-mediated development in a host-bacterial mutualism. *Science*, *306*, 1186–1188. https://doi.org/10.1126/science.1102218

Kremer, N., Philipp, E. E., Carpentier, M. C., Brennan, C. A., Kraemer, L., Altura, M. A., ... McFall-Ngai, M. J. (2013). Initial symbiont contact orchestrates host-organ-wide transcriptional changes that prime tissue colonization. *Cell Host and Microbe*, *14*, 183–194. https://doi.org/10.1016/j.chom.2013.07.006

Lee, J. C., Lee, E. J., Lee, J. H., Jun, S. H., Choi, C. W., Kim, S. I., ... Hyun, S. (2012). *Klebsiella pneumoniae* secretes outer membrane vesicles that induce the innate immune response. *FEMS Microbiology Letters*, *331*, 17–24. https://doi.org/10.1111/j.1574-6968.2012.02549.x

Lee, J. H., Jun, S. H., Kim, J. M., Baik, S. C., & Lee, J. C. (2015). Morphological changes in human gastric epithelial cells induced by nuclear targeting of *Helicobacter pylori* urease subunit A. *Journal of Microbiology*, *53*, 406–414. https://doi.org/10.1007/s12275-015-5085-5

Lee, K. L., Tsai, P. C., You, M. L., Pan, M. Y., Shi, X., Ueno, K., ... Wei, P. K. (2017). Enhancing surface sensitivity of nanostructure-based aluminum sensors using capped dielectric layers. *ACS Omega*, *2*, 7461–7470. https://doi.org/10.1021/acsomega.7b01349

Lee, R. F. S., Escrig, S., Maclachlan, C., Knott, G. W., Meibom, A., Sava, G., & Dyson, P. J. (2017). The differential distribution of RAPTA-T in non-invasive and invasive breast cancer cells correlates with its anti-invasive and anti-metastatic effects. *International Journal of Molecular Science*, *18*, e1869. https://doi.org/10.3390/ijms18091869

Lee, R. F. S., Riedel, T., Escrig, S., Maclachlan, C., Knott, G. W., Davey, C. A., ... Dyson, P. J. (2017). Differences in cisplatin distribution in sensitive and resistant ovarian cancer cells: A TEM/NanoSIMS study. *Metabolomics*, *9*, 1413–1420. https://doi.org/10.1039/c7mt00153c

Lema, K. A., Clode, P. L., Kilburn, M. R., Thornton, R., Willis, B. L., & Bourne, D. G. (2016). Imaging the uptake of nitrogen-fixing bacteria into larvae of the coral *Acropora millepora*. *ISME Journal*, *10*, 1804–1808. https://doi.org/10.1038/ismej.2015.229

Lynch, J. B., Schwartzman, J. A., Bennett, B. D., McAnulty, S. J., Knop, M., Nyholm, S. V., & Ruby, E. G. (2019). Ambient pH alters the protein content of outer membrane vesicles, driving host development in a beneficial symbiosis. *Journal of Bacteriology*, *201*, e00319–19. https://doi.org/10.1128/JB.00319-19

Maxwell, R.M., and Delaney, H.D. (2004). *Designing experiments and analyzing data*. (Mahwah, New Jersey: Lawrence Erlbaum Associates).

McFall-Ngai, M. (2014a). Divining the essence of symbiosis: Insights from the squid–vibrio model. *PLoS Biology*, *12*, e1001783. https://doi.org/10.1371/journal.pbio.1001783

McFall-Ngai, M., Hadfield, M. G., Bosch, T. C., Carey, H. V., Domazet-Loso, T., Douglas, A. E., ... Wernegreen, J. J. (2013). Animals in a bacterial world, a new imperative for the life sciences. *Proceedings of the National Academy of Sciences U S A*, *110*, 3229–3236. https://doi.org/10.1073/pnas.1218525110

McFall-Ngai, M., Heath-Heckman, E. A., Gillette, A. A., Peyer, S. M., & Harvie, E. A. (2012). The secret languages of coevolved symbioses: Insights from the *Euprymna scolopes*–*Vibrio fischeri* symbiosis. *Seminars in Immunology*, *24*, 3–8. https://doi.org/10.1016/j.smim.2011.11.006

McFall-Ngai, M. J. (2014b). The importance of microbes in animal development: Lessons from the squid–vibrio symbiosis. *Annual Reviews of Microbiology*, *68*, 177–194. https://doi.org/10.1146/annurev-micro-091313-103654

Montgomery, M. K., & McFall-Ngai, M. (1993). Embryonic development of the light organ of the sepiolid squid *Euprymna scolopes* Berry. *Biological Bulletin*, *184*, 296–308. https://doi.org/10.2307/1542448

Moriano-Gutierrez, S., Koch, E. J., Bussan, H., Romano, K., Belcaid, M., Rey, F. E., ... McFall- Ngai, M. (2019). Critical symbiont signals drive both local and systemic changes in diel and developmental host gene expression. *Proceedings of the National Academy of Sciences USA*, *116*, 7990–7999. https://doi.org/10.1073/pnas.1819897116

Musat, N., Musat, F., Weber, P. K., & Pett-Ridge, J. (2016). Tracking microbial interactions with NanoSIMS. *Current Opinions in Biotechnology*, *41*, 114–121. https://doi.org/10.1016/j.copbio.2016.06.007

Nawroth, J. C., Guo, H., Koch, E., Heath-Heckman, E. A. C., Hermanson, J. C., Ruby, E. G., ... McFall-Ngai, M. (2017). Motile cilia create fluid-mechanical microhabitats for the active recruitment of the host microbiome. *Proceedings of the National Academy of Sciences USA*, *114*, 9510–9516. https://doi.org/10.1073/pnas.1706926114

Nyholm, S. V., Deplancke, B., Gaskins, H. R., Apicella, M. A., & McFall-Ngai, M. J. (2002). Roles of *Vibrio fischeri* and nonsymbiotic bacteria in the dynamics of mucus secretion during symbiont colonization of the *Euprymna scolopes* light organ. *Applied and Environmental Microbiology*, *68*, 5113–5122. https://doi.org/10.1128/aem.68.10.5113-5122.2002

Nyholm, S. V., & Graf, J. (2012). Knowing your friends: Invertebrate innate immunity fosters beneficial bacterial symbioses. *Nature Reviews Microbiology*, *10*, 815–827.

Nyholm, S. V., & McFall-Ngai, M. J. (2004). The winnowing: Establishing the squid–vibrio symbiosis. *Nature Reviews Microbiology*, *2*, 632–642.

Nyholm, S. V., Stabb, E. V., Ruby, E. G., & McFall-Ngai, M. J. (2000). Establishment of an animal–bacterial association: Recruiting symbiotic vibrios from the environment. *Proceedings of the National Academy of Sciences USA*, *97*, 10231–10235. https://doi.org/10.1073/pnas.97.18.10231

Ruby, E. G., & Lee, K. H. (1998). The *Vibrio fischeri*–*Euprymna scolopes* light organ association: Current ecological paradigms. *Applied and Environmental Microbiology*, *64*, 805–812.

Ruby, E. G., & Nealson, K. H. (1977). Pyruvate production and excretion by the luminous marine bacteria. *Applied and Environmental Microbiology*, *34*, 164–169.

Stephens, G. C. (1988). Epidermal uptake of amino acids in marine invertebrates: Mechanisms and studies of specificity. *Biochimica et Biophysica Acta*, *947*, 113–138.

Sycuro, L. K., Ruby, E. G., & McFall-Ngai, M. (2006). Confocal microscopy of the light organ crypts in juvenile *Euprymna scolopes* reveals their morphological complexity and dynamic function in symbiosis. *Journal of Morphology*, *267*, 555–568. https://doi.org/10.1002/jmor.10422

Tai, V., Carpenter, K. J., Weber, P. K., Nalepa, C. A., Perlman, S. J., & Keeling, P. J. (2016). Genome evolution and nitrogen fixation in bacterial ectosymbionts of a protist inhabiting wood-feeding cockroaches. *Applied and Environmental Microbiology*, *82*, 4682–4695. https://doi.org/10.1128/AEM.00611-16

Takado, Y., Knott, G., Humbel, B. M., Masoodi, M., Escrig, S., Meibom, A., & Comment, A. (2015). Imaging the time-integrated cerebral metabolic activity with subcellular resolution through nanometer-scale detection of biosynthetic products deriving from ^{13}C-glucose. *Journal of Chemical Neuroanatomy*, *69*, 7–12. https://doi.org/10.1016/j.jchemneu.2015.09.003

Volland, J. M., Schintlmeister, A., Zambalos, H., Reipert, S., Mozetic, P., Espada-Hinojosa, S., ... Bright, M. (2018). NanoSIMS and tissue autoradiography reveal symbiont carbon fixation and organic carbon transfer to giant ciliate host. *ISME Journal*, *12*, 714–727. https://doi.org/10.1038/s41396-018-0069-1

Wier, A. M., Nyholm, S. V., Mandel, M. J., Massengo-Tiasse, R. P., Schaefer, A. L., Koroleva, I., ... McFall-Ngai, M. J. (2010). Transcriptional patterns in both host and bacterium underlie a daily rhythm of anatomical and metabolic change in a beneficial symbiosis. *Proceedings of the National Academy of Sciences USA*, *107*, 2259–2264. https://doi.org/10.1073/pnas.0909712107

Wollenberg, M. S., & Ruby, E. G. (2009). Population structure of *Vibrio fischeri* within the light organs of *Euprymna scolopes* squid from two Oahu (Hawaii) populations. *Applied and Environmental Microbiology*, *75*, 193–202. https://doi.org/10.1128/AEM.01792-08

Wright, S. H., & Manahan, D. T. (1989). Integumental nutrient uptake by aquatic organisms. *Annual Review of Physiology*, *51*, 585–600. https://doi.org/10.1146/annrev.ph.51.030189.003101

Zhou, Z., White, K. A., Polissi, A., Georgopoulos, C., & Raetz, C. R. (1998). Function of *Escherichia coli* MsbA, an essential ABC family transporter, in lipid A and phospholipid biosynthesis. *The Journal of Biological Chemistry*, *273*, 12466–12475. https://doi.org/10.1074/jbc.273.20.12466

SUPPORTING INFORMATION

Additional supporting information may be found online in the Supporting Information section at the end of this article.